STH/CFD COUPLED CALCULATIONS OF TWO POSTULATED PLOFA SCENARIOS IN THE NACIE-UP FACILITY

A. Pucciarelli[a*], F. Galleni[a], M. Moscardini[a], D. Martelli[b], N. Forgione[a]

[a] Dipartimento di Ingegneria Civile e Industriale, Università di Pisa, L.go Lucio Lazzarino n. 2, Pisa, Italy

[b] Experimental Engineering Division, Fusion and Technology for Nuclear Safety and Security Department ENEA Brasimone Research Centre, 40032 Camugnano (BO), Italy

[*]Corresponding author E-mail: andrea.pucciarelli@dici.unipi.it

ABSTRACT

In the present paper, coupled STH/CFD calculations are performed addressing two operating conditions in the frame of the NACIE-UP experimental campaign. In order to simulate mixed and natural circulation phenomena related to liquid metals thermal hydraulics, the RELAP5/Mod3.3 STH code and the CFD code ANSYS Fluent are adopted in an integrated manner. The combined use of STH and CFD code aims to help the user to overcome the limits of the individual techniques and thus achieving a better predicting capability with respect to each stand-alone application.

Measured values and calculated results are here discussed and compared highlighting the advantages and drawbacks of the adopted techniques. In particular, the coupled application provided the best results in terms of predicted mass flow rate and comprehensiveness of information giving the possibility to analyse the local and cross-sectional distributions. Furthermore, as additional beneficial aspect, CFD results can be used as a tuning tool for some of the STH code parameters. Coupled STH/CFD application may be consequently considered as a sound candidate for addressing liquid metal thermal hydraulics in complex geometries and large systems.

1 INTRODUCTION

The use of coupled STH/CFD calculations is becoming a sound approach for the simulation of complex thermal hydraulics analyses due to its capability addressing phenomena which may involve very different spatial and time scales, straddling from the small scales of turbulence to the ones influencing the system as a whole (Roelofs, 2019). During the last decades, System Thermal Hydraulics (STH) codes proved the capability to suitably reproduce phenomena occurring in complex systems, both for single and two-phase flows, becoming one of the most relevant tools in the licensing process of Nuclear Power Plants (NPPs). In this sense, the STH code RELAP5 was successfully used for addressing several operating and postulated accidental conditions which may occur in PWRs and BWRs reactors (see e.g. D'Auria et al., 2006).

Nevertheless, the 1D STH codes modelling approach is not able to accurately reproduce the intrinsically 3-Dimensional phenomena which may occur in large environments and complex geometries as, for instance, pool type reactors and fuel assemblies adopting wrapped wires rod bundles. Such geometrical configurations, which are absent in most of the previous Generations of NPPs, are instead a key feature of the upcoming Generation IV, specifically for the Liquid Metals Fast Breeder Reactors (LMFBRs). On the other hand, simulating 3-Dimensional complex geometries is instead one of the key features of CFD approaches; CFD simulations, however, are well known to be computationally expensive and, furthermore, lack in accuracy when considering two-phase flow conditions and phase transition. As a consequence, CFD became a sound candidate for integrating the capabilities of STH codes and to achieve a suitable accuracy level in the prediction and simulation of liquid metals thermal hydraulics.

During the last years, the University of Pisa (UniPi) in the frame of EU H2020 project SESAME, started a program for the qualification and validation of coupling techniques to be used for liquid metals thermal-hydraulics applications (see e.g. Martelli et al., 2017; Galleni et al., 2020). In particular, UniPi developed a coupled STH/CFD tool adopting the code RELAP5/Mod3.3 and the commercial software ANSYS Fluent for the STH and CFD side respectively. Similar processes were also carried out by other institutions, see e.g. the works by Toti and co-authors at SCK•CEN (Toti et al., 2018a and 2018b) and the ones by Zwijsen et al. 2019 at NRG.

In this framework, UniPi mainly focused on the simulation of two experimental facilities set at the Research Center ENEA Brasimone: the CIRCE pool (Pesetti et al., 2018) and the NACIE-UP loop (Di Piazza et al., 2016). Concerning the NACIE-UP facility, previous analyses both concerned the analysis of single components (Marinari et al., 2019) and of the whole facility, both with STH stand-alone calculations (Forgione et al, 2019) and coupled STH/CFD 2D applications. More recently, CFD analyses were also performed to obtain better information about the addressed facilities and thus impose improved boundary conditions and parameters for the STH applications (see e.g. Buzzi et al., 2020 and Pucciarelli et al., 2020). Specifically, in the work Pucciarelli et al., 2020, CFD was adopted in order to obtain a better estimation of the distributed pressure drops in the NACIE-UP Fuel Pin Simulator (FPS) component.

As following step, the present work aims at performing STH/CFD calculations of the whole facility, this time considering a 3-Dimensional environment for the CFD domain. Measured values are compared with the calculated results showing the improved capabilities of coupled tools. The beneficial influence of CFD as a tuning tool for some of the relevant parameters of STH codes is also highlighted, suggesting that an integrated STH/CFD approach could be a valid tool for the resolution of wide and complex thermal hydraulics systems.

2 NACIE-UP FACILITY DESCRIPTION AND DISCRETIZATION

Facility description

In the present paper, the NACIE-UP facility (NAtural CIrculation Experiment – UPgraded, Di Piazza et al., 2016), set in Brasimone RC is considered. It is designed in support of the development of LMFBRs and its main aim is the investigation of forced and mixed circulation phenomena connected with the use of liquid metals, specifically LBE (Lead Bismuth Eutectic). It consists of a rectangular loop equipped with a Fuel Pin Simulator (FPS) and a Heat Exchanger; a sketch of the facility is reported in Figure 1. The FPS represents the hot sink of the system whilst the heat exchanger, where cooling water flows on the secondary side, represents the cold one. In order to promote natural circulation phenomena, the two devices are allocated at a significantly different height. Furthermore, circulation is also enhanced through the injection of Argon at the base of the Riser; the inert gas is then collected in the Expansion Vessel. Varying the Argon mass flow rate, it is possible to impose a defined flow regime and to simulate operating and accidental conditions. Besides, Argon also works as cover gas in the expansion vessel, thus reducing the occurrence of LBE oxidation.

The Fuel Pin Simulator (FPS), located at the bottom of the hot leg, consist of 19 electrically heated pins arranged in a hexagonal lattice; the duct has an hexagonal shape too (Figure 2a). It is 1.3 m long, nevertheless, only 600 mm are actually heated (Figure 2b). Upstream the heated section, a 615 mm long unheated entrance region is located assuring fully developed flow condition in the heated section itself; downstream, a 115 mm discharge unheated region is also located. The correct positioning of the pins is maintained using wires wrapped around each pin (represented by black circles in Figure 2) and by two grids, one upstream and the other downstream the FPS. Pins and wires define 54 subchannels, some of which are instrumented. In particular, in the present paper, the experimental temperature measurements on the wall of Pin 3 (see the red dot in Figure 2) and for subchannel S5 are considered for comparison with the calculated results. Comparison between measured and calculated values is performed also for the mass flow rate (measured by a thermal mass flow meter) and for the temperature values measured upstream and downstream the Fuel Pin Simulator.

Facility discretization

The facility discretization procedure for the coupled STH/CFD application consisted into two main phases: the former is the nodalization to be adopted by the stand alone STH code RELAP5/Mod3.3, the latter is the introduction of the CFD domain generated for the FPS in the existing STH nodalization. RELAP5/Mod3.3 (RELAP5 Code Manual, 2001) is a modified version of the RELAP5 code which allows the analysis of thermal hydraulic phenomena involving liquid metals. The thermodynamic properties of LBE were implemented according to the work by Sobolev's (Sobolev,2011), heat transfer correlations for liquid metals (see e.g. Ushakov, 1977 and Seban and Shimazaki, 1951) were implemented as well; the code was qualified in the frame of previous works performed at UniPi involving both STH stand-alone (Forgione et al., 2019) and coupled STH/CFD calculations (Martelli et al., 2017).

RELAP5 Nodalization

For the first phase, the existing nodalization designed at UniPi (Forgione et al., 2019) was retained and updated. A sketch of the considered nodalization is depicted in Figure 3. It consists in a series of pipes and branches subdivided into two circuits: the primary loop, where LBE flows, and the secondary loop, where water flows which represents the shell side of the heat exchanger. Heat transfer between the two loops is assured by the thermal structures connected to Pipes 190 and 590; a heated structure simulating the heating rods is also located in correspondence of Pipe 110, which corresponds to the heated part of the FPS. The Time Dependent Volume (TDV) 410 and the Time Dependent Junction (TDJ) 405 represent the Argon Injection System: Argon is supplied downstream the FPS and later separated at Branch 150 and collected at TDV 320, which also represents the cover gas region and allows imposing the pressure boundary condition. The presently adopted nodalization updates some of the pressure drop coefficients used by Forgione et al., 2019 in their work; specifically, it adopts distributed pressure drop coefficients for the FPS region derived by CFD calculations performed by Pucciarelli et al., 2020. Indeed, owing to the presence of rod bundles and wrapped wires, a single pressure drop coefficient may not be suitable for a good representation of the involved phenomena. As a consequence, CFD calculations were performed for a sufficiently wide range of operating conditions, straddling from laminar to fully turbulent flows; pressure drops along the FPS region were calculated and discussed on the basis of the corresponding Reynolds number. The obtained results reported a good matching with the Cheng and Todreas (Chen et al., 2018) correlation which was consequently implemented in the code and adopted for Pipes 100, 110 and 120

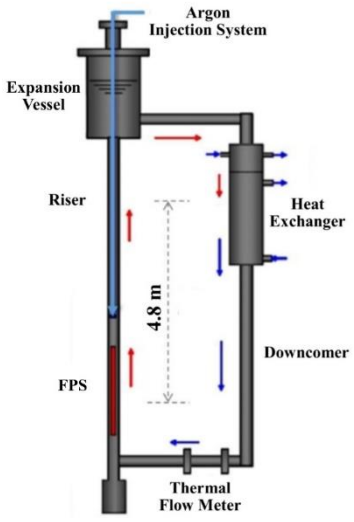

Figure 1: Schematic layout of the NACIE-UP facility, Di Piazza et al., 2016.

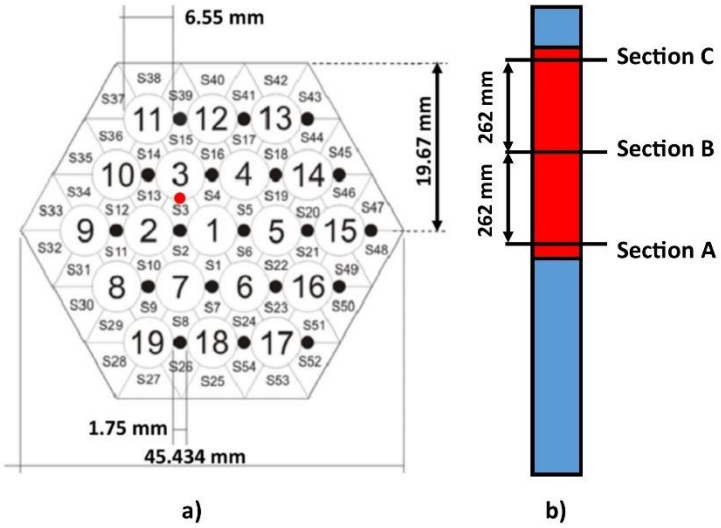

Figure 2: Sketch of the cross section of the FPS, Di Piazza et al. 2016 (a) and its axial subdivision (b); the heated length is depicted in red.

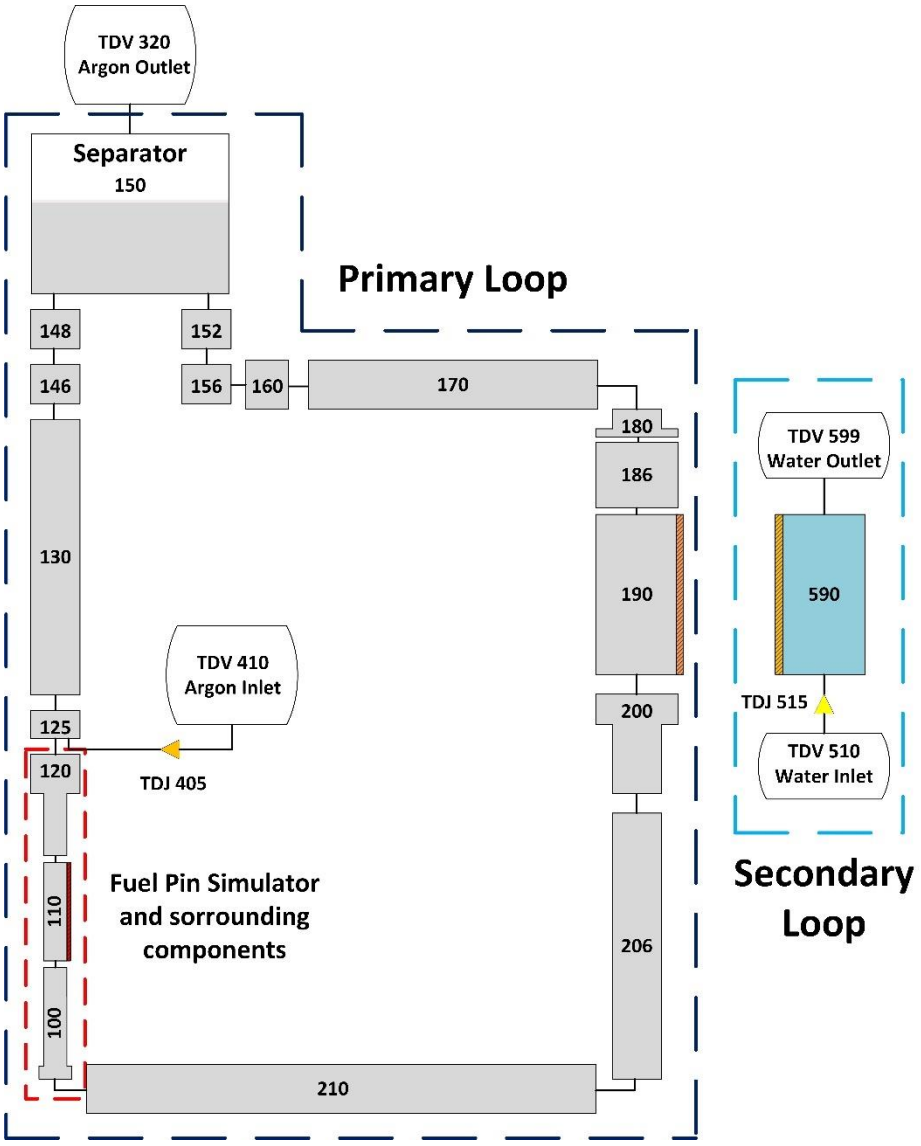

Figure 3: Adopted RELAP5/Mod3.3 stand-alone nodalization.

CFD Nodalization

The second phase foundation was the work by Pucciarelli et al.2010, which focused on the CFD analysis of thermo-fluid-dynamic phenomena occurring in the FPS of the NACIE-UP facility. The work also concerned the prediction and comparison of the calculated temperature distribution with the experimental measurements, reporting a good matching. The considered geometry is reported in Figure 4; the same strategies and parameters adopted by Pucciarelli et al., 2020 for the mesh generation were adopted here and are reported in Table 1, the commercial code ANSYS Fluent (ANSYS, 2018) was used for the present simulations, too. The obtained mesh, of which a detail is reported in Figure 5, is highly refined nearby the walls, especially in the region of the wrapped wires. This allows the use of low Reynolds turbulence models, providing a y^+ value lower than unity for the first cells close to the wall. The selected turbulence model is the SST k-ω (Menter, 1994) which proved good capabilities in predicting heat transfer phenomena in previous works (see e.g. Roelofs, 2019, Pucciarelli et al., 2020),. As it can be observed from Figure 5, in order to reduce the computational cost, the

heating rods were modelled reproducing only the external layer; thermal power is consequently supplied imposing heat flux on the internal surface of the rods. This assumption was considered following the previous work Pucciarelli et al., 2020 in which steady-state analyses of the presently addressed facility were performed. Nevertheless, thermal inertia is a relevant feature to be reproduced to obtain suitable predictions in transient applications; as a consequence, the density of the solid material was slightly increased with the aim to match the simulated and actual heat capacity of the rods.

Table 1: Parameters adopted for the creation of the CFD nodalization in ANSYS Fluent.

Fluid Domain	
Base size [mm]	1
Local Minimum size [mm]	0.2
Curvature Normal Angle [°]	8
First Layer Thickness [mm]	0.01
Maximum Layers	5
Growth Rate	1.7
Solid Domain	
Base size [mm]	1
Local Minimum size [mm]	0.5
Curvature Normal Angle [°]	8
Total N° of cells (millions)	28.5

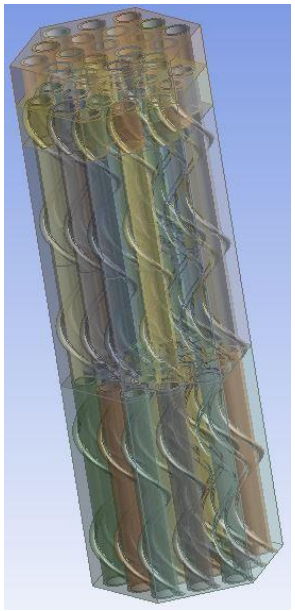

Figure 4 Considered Geometry.

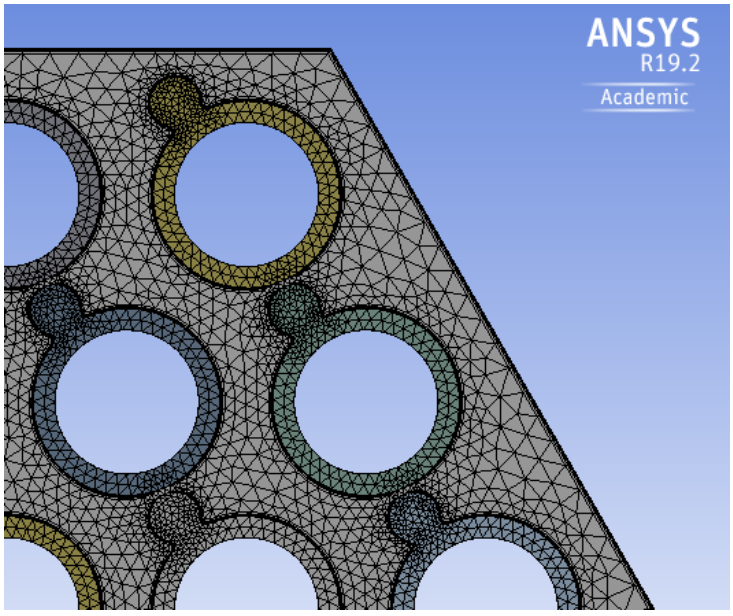

Figure 5: Detail of the obtained CFD nodalization.

Coupled Nodalization

The obtained STH and CFD nodalization were subsequently integrated to obtain the nodalization to be adopted for the coupled STH/CFD calculation. The non-overlapping approach was selected in the present work; as a consequence, each code solves its domain without any geometrical superimposition. In particular, CFD solves the 3-dimensional environment of the FPS while RELAP5/Mod3.3 deals with all the other components of the experimental loop; the RELAP5 nodalization was consequently modified to be suitable for the coupling with the CFD domain. Figure 5 shows a magnification of the region surrounded by a dashed red line in Figure 3, the red zone in contact with the component 110 represents the FPS region in the STH stand-alone nodalization. Figure 7 reports instead of the updated nodalization for the coupled STH/CFD application with the variables to be exchanged at the codes interfaces. It can be observed that the components from Pipe 100-3 to Pipe 120-1, which refer to hexagonal duct, were removed and substituted by the CFD domain. On the other hand, two Time Dependent Volumes, TDV 112 and TDV 108, and a Time Dependent Junction, TDJ 115, were introduced in order to provide suitable boundary conditions to the STH portion of the nodalization. Specifically, TDV 112 is used for imposing the Temperature calculated at the outlet of the CFD domain, TDV 108 for the Pressure at the basis of the FPS and TDJ 115 for mass flow rate at the outlet end of the FPS.

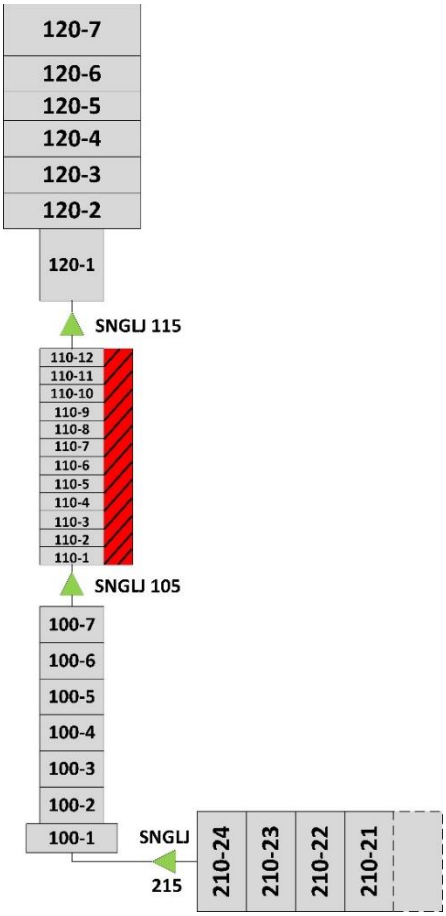

Figure 6: Adopted RELAP5/Mod3.3 stand-alone nodalization, particular of the FPS region.

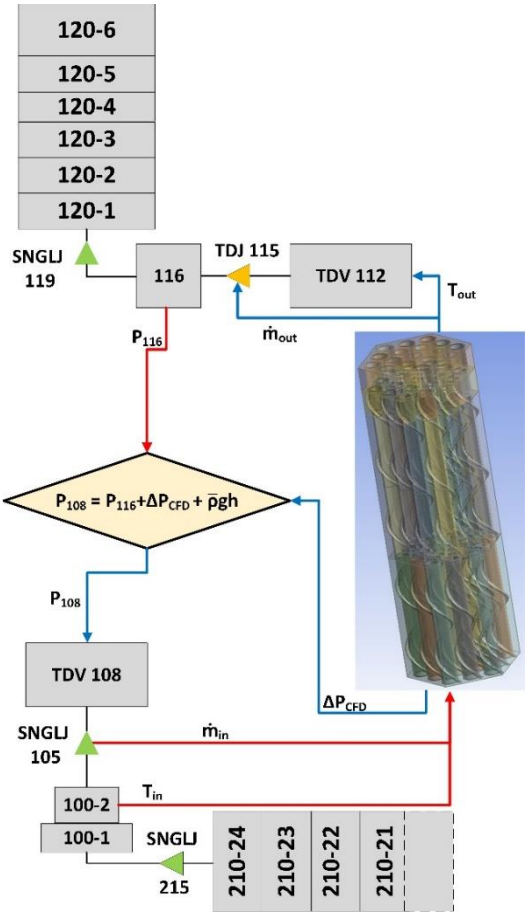

Figure 7: Adopted coupled calculation nodalization, particular of the FPS region and data transfer scheme.

CFD receives instead the imposed mass flow inlet from the Single Junction SNGJ-105 and the Inlet Temperature from Pipe 100-2; at the outlet section a constant pressure is instead imposed. Maintaining the pressure at a constant reference value inside the CFD domain, variations of the pressure field are limited in each iteration and computational cost is reduced. CFD is consequently used for calculating the pressure drops and the pressure head across the FPS component; these data are combined with the pressure calculated by the STH code in Pipe 116 to then be fed back to TDV 108, which impose the pressure value on the STH nodalization.

The implicit scheme is adopted for the time advancement of the coupled calculation; synchronization is instead assured at defined time levels. CFD moves between the time levels considering a single time-step, the STH code instead subdivides the same interval into several time-steps, depending on its requirements for the fulfilment of the Courant limit. At each time-step, CFD first performs its calculation based on the information of the previous time-step; the updated results are provided to the STH codes which consequently performs its calculation. CFD and STH results are then compared; if the convergence criteria imposed by the user are fulfilled, the calculation moves to the following time step, if not the same time level is repeated with updated boundary conditions. Under-relaxation for time-step internal iteration is also considered to improve the robustness and convergence capability of the coupled application.

3 RESULTS

The obtained results are discussed in the present section. Table 2 resumes the considered operating conditions, FT1 takes into account an argon mass flow transition, while FT3 reproduces a postulated PLOFA with both Argon, secondary water transition and a decrease of the supplied power at the FPS (Di Piazza et al., 2017).

Table 2: Considered Operating Conditions.

Case		ṁ Argon [Nl/min]	Q_{FPS} [kW]	Secondary Water ṁ [m^3/h]	Secondary Water T_{in} [m^3/h]
Fundamental Test 1 FT1	Before	20	50	10	170
	After	10	50	10	170
Fundamental Test 3 FT3	Before	20	100	10	170
	After	0	10	6.6	170

Figure 8 reports the comparison of the calculated and measured LBE mass flow rate trends for the first 250 s of transient FT1; the abrupt decrease experienced at the beginning is directly connected with the sudden reduction of the Argon supplied by the injection system. As it can be observed, the coupled calculation performs better in comparison to the STH stand-alone application; in particular, after 50 s, the predicted trend lays inside the experimental uncertainty range. A steeper reduction of the predicted mass flow rate concerning the measured one is observed. This could be due to approximations introduced by correlations of the adopted models resulting unsuitable to perfectly reproduce two-phase flows characterized by relevant amounts of transported incondensable gases (Issa and Galleni, 2015). Nevertheless, the obtained result is fairly good and the transient experimental trend was reproduced. Besides, the slight improvement of the present RELAP5 stand-alone prediction with respect to the results obtained in the previous work Forgione et al., 2019 must be observed as well. This behaviour is mainly related to the pressure drop coefficients presently implemented in the FPS region and updated based on CFD calculations (Pucciarelli et al., 2020); this is another hint of the mutual advantages that may be provided by the combined use of STH and CFD codes.

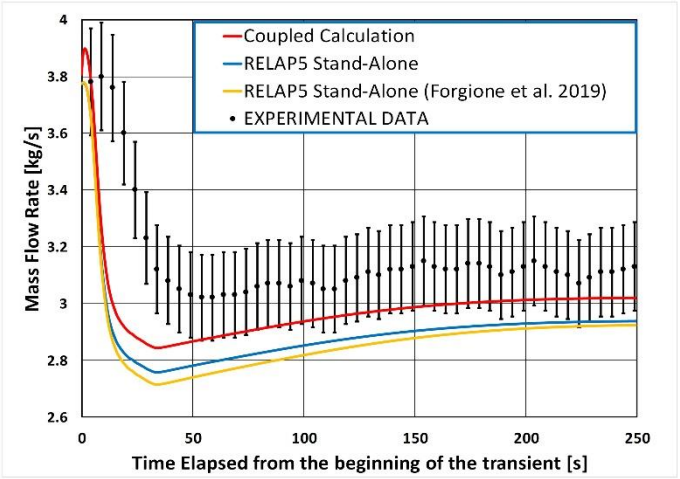

Figure 8: FT1 – numerical and experimental mass flow rate.

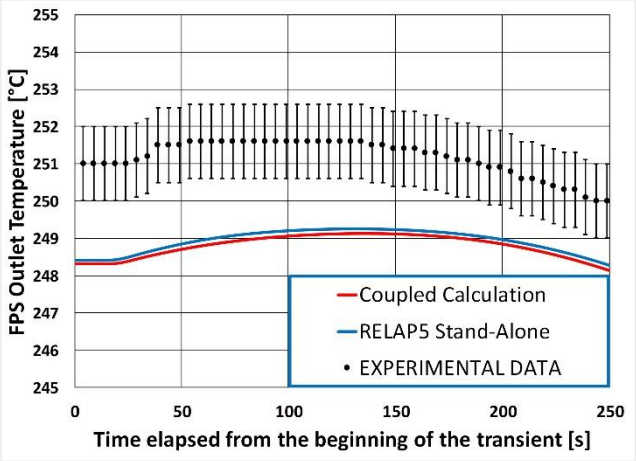

Figure 9: FT1 – numerical and experimental bulk temperature at the inlet of the FPS.

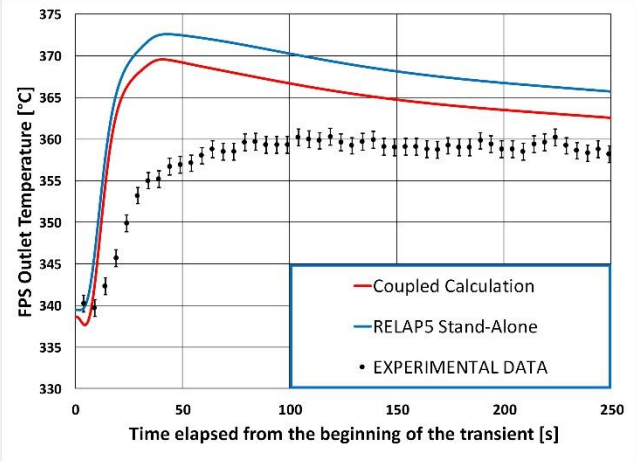

Figure 10: FT1 – numerical and experimental bulk temperature at the outlet of the FPS.

Figure 9 reports the predicted and measured temperature trends at the inlet section of the Fuel Pin Simulator; as it can be noted the observed phenomenon has been both qualitatively and quantitatively well reproduced, the predicted temperatures, indeed, underestimate the measured temperature trend of just 2-3°C. Figure 10 reports instead of the correspondent temperature trends at the outlet of the FPS component. Coherently with the predicted LBE mass flow rate, the calculated temperature trends slightly overestimate the measured values. Again, it is worth highlighting the better prediction provided by the coupled calculation.

Figure 11 shows the comparison between the calculated and measured mass flow rates for case FT3. Results provided by the Coupled calculation and the presently performed RELAP5 Stand-Alone application are almost superimposed and, after 50 s from the beginning of the transient, very close to the measured values. The performance is superior with respect to the previous results by Forgione et al., 2019 which slightly underestimated the measured values for a longer time interval. It is again stressed that the better trends provided by the presently performed RELAP5 Stand-Alone calculation are related to the improved pressure drop coefficients obtained via the CFD analyses of the Fuel Pin Simulator performed by Pucciarelli et al. 2010. Concerning the abrupt decrease experienced at the beginning, it is again remarked that the different behaviour with respect to the experimental measurements is likely to be due to the intrinsic uncertainties of the regime maps adopted by RELAP5 which may not be completely suitable for the LBE-Argon two-phase flow.

Figure 12 and Figure 13 show the comparison between the measured and calculated results for the temperature trends at the inlet and outlet section of the Fuel Pin Simulator, respectively. The inlet temperature trends are predicted very well; indeed, as it happened for the previous FT1 case, they differ from the measured values by just 2-3°C. Concerning the outlet temperature, instead, the underestimation is slightly larger, though coherent with the predicted mass flow rates; the larger discrepancies observed at the beginning of the transient are clearly connected with the different predicted behaviour of the mass flow rate in the region 25-50 s. The overall result is fairly good, in particular, if Figure 14 and Figure 15 are also taken into account. They report the comparison between the measured and calculated temperature trends for some selected thermocouples located inside the FPS. Specifically, they are positioned at different axial sections (A, B and C, see Figure *2*b for

context): the ones in Figure 14 in the bulk region of channel S5, the ones in Figure 15 are instead located on the wall of Pin 3 (see Figure 2a for reference). It is also remarked that these comparisons may be obtained only performing coupled calculations; indeed, STH codes stand-alone applications cannot provide such information because of the intrinsic limits of their modelling approach. The obtained results match very well the measured values for all the considered sections suggesting that the assumptions regarding the thermal inertia of the pins were sufficiently correct.

Another result that could not be obtained by STH stand-alone calculations is the cross-sectional distributions reported in Figure 16 and Figure 17 at two selected time levels. Thanks to the CFD contribution, the coupled application may provide detailed representations of the instantaneous distribution of relevant quantities in the corresponding domain. In the cited figures, temperature distributions are shown, reporting the presence of two temperature regions: a hotter region in the very internal rank and a colder region outside the outer rank Pins. Together with the temperature trends reported in Figure 14 and Figure 15, this information may clearly help to identify the region that may undergo the most severe conditions.

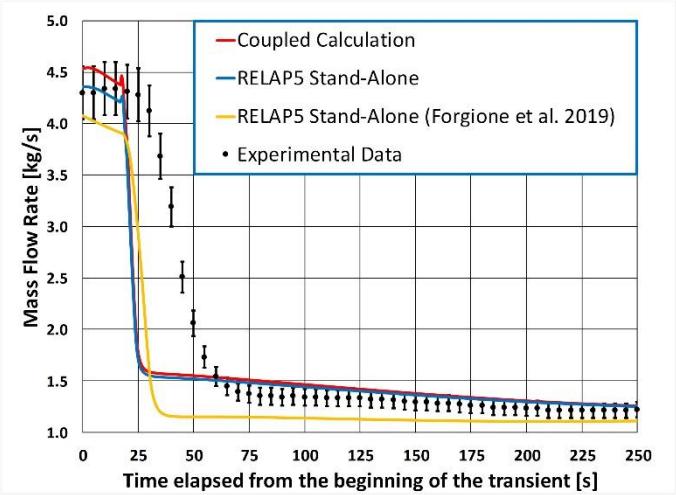

Figure 11: FT3 – numerical and experimental mass flow rate.

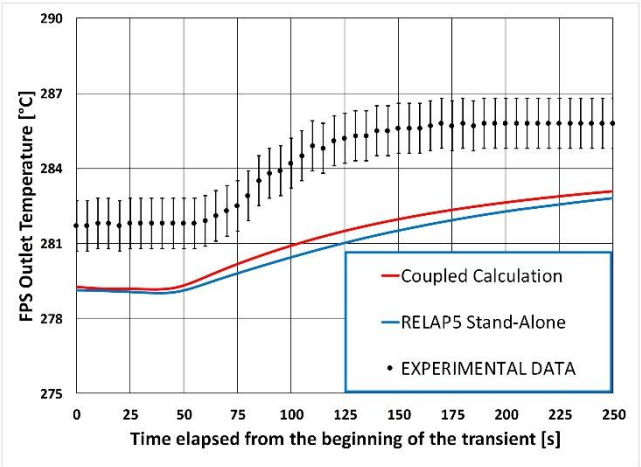

Figure 12: FT3 – numerical and experimental bulk temperature at the inlet of the FPS.

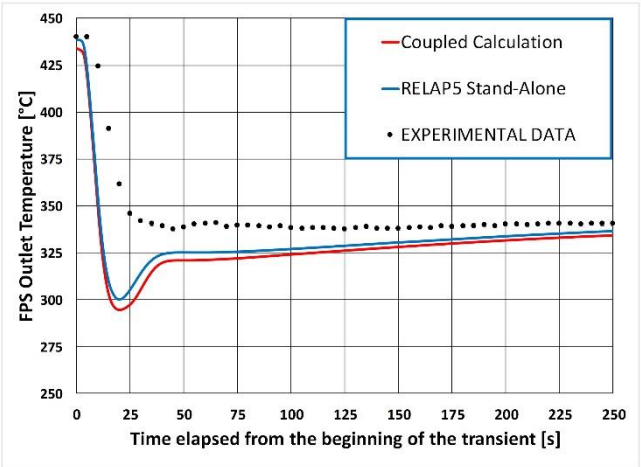

Figure 13: FT3 – numerical and experimental bulk temperature at the outlet of the FPS.

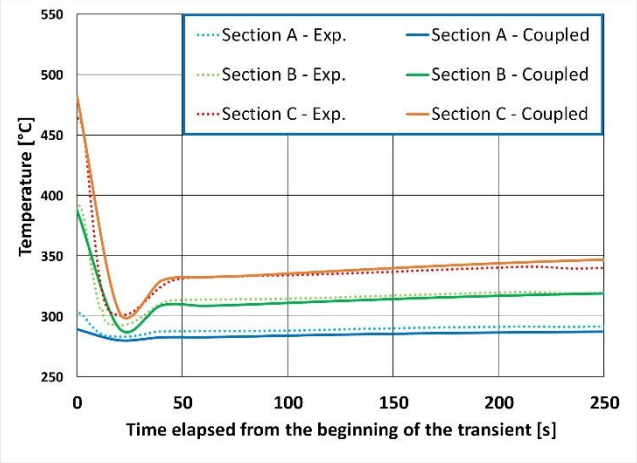

Figure 14: FT3 – numerical and experimental bulk temperature for S5 at three selected sections.

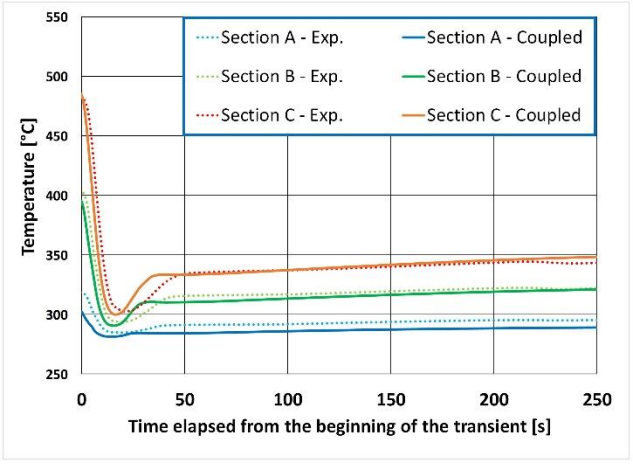

Figure 15: FT3 – numerical and experimental wall temperature for Pin 3 at three selected sections.

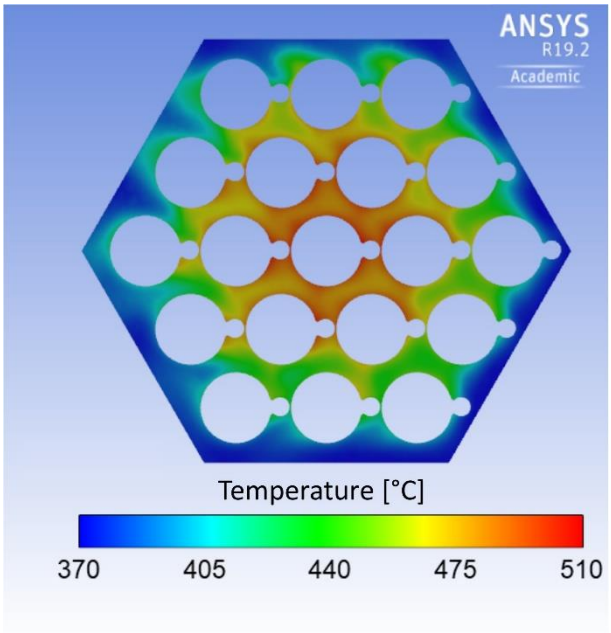

Figure 16: Temperature distribution at Section C of the FPS at the beginning of the analysed transient (t=0 s).

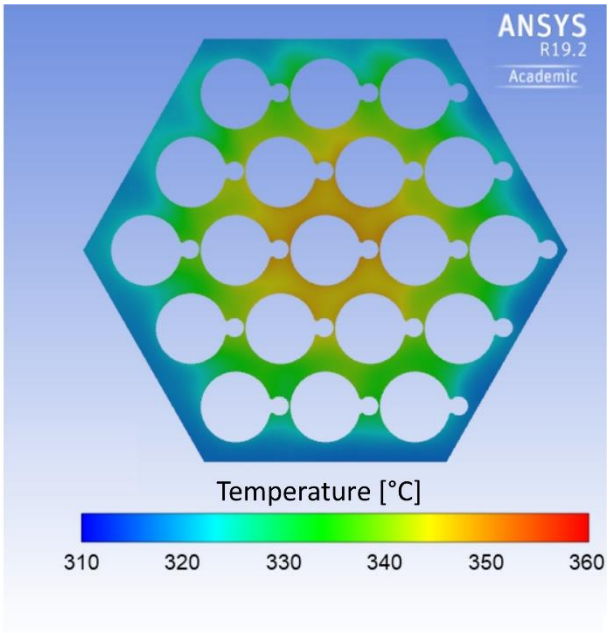

Figure 17: Temperature distribution at Section C of the FPS after 260 s from the beginning of the analysed transient.

4 CONCLUSIONS

In the present paper, two experimental conditions addressed in the NACIE-UP facility were considered and reproduced performing STH/CFD coupled calculations. The experimental facility was firstly simulated via STH stand-alone calculations in which some of the parameters were tuned taking into account CFD calculations performed in previous works. Coupled calculations were later performed with the introduction of the CFD domain adopting a non-overlapping approach and an implicit time-advancing scheme.

Numerical and experimental results were compared showing the good predicting capabilities of the adopted techniques. With respect to the considered STH attempts, the coupled calculation provided better results, in particular for case FT1, in which the predicted mass flow rate lays inside the experimental uncertainty range. Improvements were also observed for the presently performed "CFD-tuned" STH calculation, which managed to reproduce results very close to the ones provided by the coupled calculation. This suggests that the integration of STH and CFD techniques may be very advantageous and, even without performing coupled calculations, the CFD may provide relevant information allowing for a sound improvement of the results obtained by STH codes.

Furthermore, the use of CFD should not be completely avoided for conditions involving intrinsically 3D environments such as pools or wire-wrapped rod bundles in which the lumped parameter approach of STH could not be the most suitable for the achievement of reliable predictions. The use of coupled calculations, even if more computationally expensive, may also provide the user with plenty of information about temperature and properties distributions inside the CFD domain. As reported in the paper, indeed, CFD allowed the calculation of temperature trends for both bulk and wall regions resulting in a good matching with the experimental data. Together with local temporal trends, CFD may also provide detailed cross-sectional distributions allowing for a better comparison of the involved global phenomena.

As a final comment, coupled calculations may really improve the present understanding and predicting capabilities of thermal-hydraulic phenomena. Indeed, when addressing systems and phenomena with different spatial and temporal time scales, the use of STH stand-alone codes may provide only limited results; CFD, instead, could help in introducing more appropriate spatial and temporal discretizations for regions and phenomena for which the 1D approach is not reliable at all. As highlighted in the present paper, the coupled STH/CFD calculation techniques seem sufficiently mature for addressing even complicated geometries and conditions, becoming a sound candidate for the simulation of the thermal-hydraulic phenomena that may be involved in innovative nuclear power plants reactors.

5 ACKNOWLEDGEMENTS

This work was performed in the framework of the H2020 SESAME project. This project has received funding from the Euratom research and training program 2014.2018 under grant agreement No 654935.

6 REFERENCES

ANSYS, Inc., "ANSYS Fluent User's Guide, Release 19.2", August 2018.

Buzzi, F., Pucciarelli, A., Galleni, F., Tarantino, M., Forgione, N., 2020, "Analysis of thermal stratification phenomena in the CIRCE-HERO facility". Annals of Nuclear Energy, Volume 131, June 2020, 107320.

Chen, S.K.,Chen, Y.M.,Todreas, N.E., 2018.The upgraded Cheng andTodreas correlation for pressure drop in hexagonal wire-wrapped rod bundles. Nucl. Eng. Des. 335, 356–373.

D'Auria, F., Salah, A.B., Petruzzi, A., Del Nevo, A., 2006. "State of the art in using best estimate calculation tools in nuclear technology". Nucl. Eng. Technol. 38, 11-32.

Di Piazza, I., Angelucci, M., Marinari, R., Tarantino, M., Forgione, N., 2016, "Heat transfer on HLM cooled wire-spaced fuel pin bundle simulator in the NACIE-UP facility". Nucl. Eng. Des. 300, 256-267.

Di Piazza, I., Angelucci, M., Polazzi, G., Sermenghi, V., 2017, "D4.10 – NACIE-UP data for PLOFA experiment". Deliverable SESAME – 654935 – D4.10 – version 0 issued on 01/09/2017.

Forgione, N., Martelli, D., Barone, G., Giannetti, F., Lorusso, P., Hollands, T., Papukchuev, A., Polidori, M., Cervone, A., Di Piazza, I., 2019, "Post-test simulations for the NACIE-UP benchmark by STH codes". Nucl. Eng. Des. 353 (2019) 110279.

Galleni, F., Barone, G., Martelli, D., Pucciarelli, A., Lorusso, P., Tarantino, M., Forgione, N., 2020, "Simulation of operational conditions of HX-HERO in the CIRCE facility with CFD/STH coupled codes". Nucl. Eng. Des. In press, https://doi.org/10.1016/j.nucengdes.2020.110552.

Issa, R. and Galleni, F., 2015, "Mechanistic simulation of slug flow in vertical pipes using the one-dimensional two-fluid model". Multiphase Science and Technology, 27(2-4): 229-245 (2015).

Marinari, R., Di Piazza, I., Tarantino, M., Angelucci, M., Martelli, D., 2019, "Experimental tests and post-tests analusis on non-uniformly heated 19-pins fuel bundle cooled by Heavy Liquid Metal". Nucl. Eng. Des. 343 (2019) 166-177.

Martelli, D., Forgione, N., Barone, G., Di Piazza, I., 2017, "Coupled simulations of the NACIE facility using RELAP5 and ANSYS FLUENT codes". Annals of Nuclear Energy 101 (2017), 408-418.

Menter, F.R., 1994. Two-equation eddy-viscosity turbulence modelling for engineering applications. AIAA J. 32 (8), 1598–1605.

Pesetti, A., Forgione, N., Narcisi, V., Lorusso, P., Giannetti, F., Tarantino, M., 2018, "ENEA CIRCE-HERO test facility: geometry and instrumentation description", ENEA report for Project H2020 SESAME WP5.2, Ref CI-I-R-343.

Pucciarelli, A., Barone, G., Forgione, N., Galleni, F., Martelli, D., 2020, "NACIE-UP post test simulations by CFD codes". Nucl. Eng. Des. 356 (2020) 110392.

RELAP5 Code Manual, 2001, "RELAP5/Mod3.3 code manual Volume I: Code structure, System models and solution methods". Nuclear Safety Analysis Division; Information System Laboratories, Inc., Rockville, Maryland Idaho Falls, 2001.

Roelefs, F., "Thermal Hydraulics Aspects of Liquid Metal Cooled Reactors", Woodheat Publishing, ISBN: 978-0-08-101981-8 (online), 2019.

Seban, R.A. and Shimazaki, T.T., 1951, "Heat Transfer to a Fluid Flowing Turbulently in a Smooth Pipe with Walls at Constant Temperature", Transactions of the American Society of Mechanical Engineers, Vol. 73, pp. 803-809.

Sobolev, V. (2011), Database of Thermophysical Properties of Liquid Metal Coolants for GEN-IV, SCK•CEN report BLG-1069, Mol, Belgium, December 2010 (rev. December 2011).

Toti, A., Vierendeels, J., Belloni, F., 2018a, "Extension and application on a pool-type test facility of a system thermal-hydraulic/CFD coupling method for transient flow analyses". Nucl. Eng. Des 331 (2018) 83-96.

Toti, A., Vierendeels, J., Belloni, F., 2018b, "Coupled system thermal-hydraulic/CFD analysis of a protected loss of flow transient in the MYRRHA reactor". Annals of Nuclear Energy 118 (2018) 199-211.

Ushakov, P.A., Zhukov, A.V., Matyukkhin, N.M., 1977. "Heat transfer to liquid metals in regular arrays of fuel elements. High Temperature 15, 868-873, translated from Teplofizika Vysokikh Temperatur, Vol. 15, No 5, pp. 1027-1033.

Zwijsen, K., Martelli, D., Breijder, P.A., Forgione., N., Roelofs, F., 2019, "Multi-scale modelling of the CIRCE-HERO facility". Nucl. Eng. Des. 335, 15 December 2019, 110344.